

---

# PromptPose: Language Prompt Helps Animal Pose Estimation

---

Xu Zhang<sup>1</sup>, Wen Wang<sup>2</sup>, Zhe Chen<sup>1</sup>, Jing Zhang<sup>1</sup>, Dacheng Tao<sup>3,1</sup>

<sup>1</sup>The University of Sydney, Australia

<sup>2</sup>University of Science and Technology of China, China

<sup>3</sup>JD Explore Academy, China

xzha0930@uni.sydney.edu.au, wangen@mail.ustc.edu.cn, zhe.chen1@sydney.edu.au  
jing.zhang1@sydney.edu.au, dacheng.tao@gmail.com

## Abstract

Recently, animal pose estimation is attracting increasing interest from the academia (e.g., wildlife and conservation biology) focusing on animal behavior understanding. However, currently animal pose estimation suffers from small datasets and large data variances, making it difficult to obtain robust performance. To tackle this problem, we propose that the rich knowledge about relations between pose-related semantics learned by language models can be utilized to improve the animal pose estimation. Therefore, in this study, we introduce a novel PromptPose framework to effectively apply language models for better understanding the animal poses based on prompt training. In PromptPose, we propose that adapting the language knowledge to the visual animal poses is key to achieve effective animal pose estimation. To this end, we first introduce textual prompts to build connections between textual semantic descriptions and supporting animal keypoint features. Moreover, we further devise a pixel-level contrastive loss to build dense connections between textual descriptions and local image features, as well as a semantic-level contrastive loss to bridge the gap between global contrasts in language-image cross-modal pre-training and local contrasts in dense prediction. In practice, the PromptPose has shown great benefits for improving animal pose estimation. By conducting extensive experiments, we show that our PromptPose achieves superior performance under both supervised and few-shot settings, outperforming representative methods by a large margin. The source code and models will be made publicly available.

## 1 Introduction

Animal pose estimation aims to locate and identify a series of animal body keypoints from an input image. It plays a key role in animal behavior understanding, zoology and wildlife conservation that can help study and protect animals better. Although the animal pose estimation task is analogous to human pose estimation [35] to some extents, this task suffers from much smaller datasets available for training. Image data of animals, especially for rare animal species, are difficult to collect and label. In addition, the visual patterns of animal poses generally have extremely large variances, including but not limited to: (1) differences in the textures of the same joints in different animals, *e.g.*, the joints of chimps and monkeys are wrinkled and hairy, while those of hippos are smooth and hairless; (2) differences in structures, *e.g.*, horses and monkeys have inherently different pose patterns; and (3) differences in poses even for the same species, *e.g.*, pandas can have various poses like standing, crawling, sitting and lying down. These challenges require the animal pose estimation model to be robust against large data variance, which is particularly difficult when the training data for animal pose estimation is scarce.

Recently, Yu et al. [32] attempted to alleviate this problem by presenting the largest animal pose estimation dataset, i.e., AP-10K, which contains 10K images from 23 animal families and 54 species. They show promising results by benchmarking different representative pose estimation methods, such as the SimpleBaseline [30] and HRNet [29], on the AP-10K dataset. Nevertheless, the performance still falls behind the one in human pose estimation, especially for some rare species and under the few-shot learning setting. This is probably due to the fact that there are too many animal species while the data volume of AP-10K is much smaller than that of the human pose estimation dataset by an order of magnitude. As a result, it is quite challenging to obtain a powerful animal pose estimation model through common training schemes. Although ImageNet pre-training helps the model converge fast, the advantage becomes marginal when training the model from scratch for a longer time as shown in [32]. Besides, although transferring the knowledge of human pose estimation models to the animal pose ones could be helpful as demonstrated in [32], the benefit is still limited due to great domain gap between human pose data and animal pose data and the lack of an explicit transfer mechanism beyond loading the pre-trained weights.

To address the challenging animal pose estimation task, we propose that the semantics encoded within well-trained language models can deliver great benefits in facilitating the understanding of animal poses. In particular, recent research on Contrastive Language-Image Pre-training (CLIP) that uses 400 million text-image paired data acquired online to train a multi-mode pre-training model shows strong ability to deal with data variance in visual tasks. Despite complicated patterns in computer vision, the CLIP can help achieve effective few-shot or even zero-shot classification by simply exploring the relations between text features and image features with the help of prompt training [20]. Motivated by the success of the CLIP for semantic relation modeling, we propose to use the CLIP-based language models to aid the estimation of animal poses with large variances, even without rich training data.

In this study, we propose a novel PromptPose framework to achieve language-model driven animal pose estimation based on prompt training. In PromptPose, we propose that adapting the language knowledge to the visual animal poses is key to exploit rich pre-trained language knowledge for effective animal pose estimation. To this end, we devise the following novel components for the PromptPose. Firstly, considering that different joints of pose keypoints are often correlated [17] due to the anatomical bone structure and kinematics and such correlation can be helpful for pose estimation, we propose a simple but effective prompt encoder to encode such joint correlation within the text features of keypoints to construct a strong language prompt. Then, we attempt to establish dense connections between text and image features by introducing a pixel-level text-image contrastive loss. The established connections can help constrain that text features and pixel-level image features are in a compatible multi-modal embedding space. In addition, we found that existing CLIP-based language models [26] primarily matches the semantics between text and image in a global manner, which may suffer from the significant gap between the global semantics and the established pixel-level local semantics. To address this issue, we further propose a semantic-level text-image contrast loss to bridge the gap between global semantics encoded within the pre-trained language model and local visual features of keypoints.

In summary, the contribution of this paper is three-fold:

- We propose a novel PromptPose framework to effectively apply language models for better estimating the animal poses based on prompt training.
- We propose semantic-level and pixel-level text-image contrastive losses, which are used to reduce the gap between the semantics of text and image in the embedding space and establish dense connections between them, respectively. A prompt encoder is also introduced to emphasize the correlation within different text keypoint embeddings to enhance the prompt.
- Experiments on two settings, i.e., 1) training on the AP-10K dataset and 2) pre-training on the MS COCO human pose dataset and finetuning on AP-10K, both demonstrate the effectiveness of the proposed PromptPose method through both supervised learning and few-shot learning.

## 2 Related work

### 2.1 Pose estimation

Pose estimation is a compelling and active research area in computer vision. Existing methods can be roughly categorized as top-down [7, 25, 19, 29, 30, 33], and bottom-up [4, 24, 10] methods. While the former detects the body instance before locating keypoints, the latter first locate identity-free keypoints then group them into pose instances. In recent years, animal pose estimation is drawing increasing attention [32, 15, 11, 22, 3], due to its wide applications including animal behavior understanding and wildlife conservation. Although most pose estimation methods are originally developed on humans, they can be directly applied to animals by simply redefining the body keypoints [32]. However, dataset for animal pose estimation are often more difficult due to large appearance variance among different animal species and the small volume of labelled animal data. For example, several datasets only concern the pose estimation of a single species like horse [22], zebra [11], and tiger [15]. The Animal Pose Dataset contain only 5 different species with limited number of image samples. Although the largest exiting animal pose estimation dataset, i.e., AP-10K [32], covers 23 animal families of 54 species, the number of training images is still smaller than the common human pose estimation dataset [18] by an order of magnitude.

To tackle this issue, previous methods resort to domain adaptation or knowledge distillation for animal pose estimation [23, 14, 28, 3, 32]. For example, Cao et al. [3] propose a cross-domain adaptation method, which transfers the knowledge in labeled human data to handle the unlabeled animal data. Similarly, Li et al. [14] utilizes domain adaptation from synthetic to real data for animal pose estimation. Yu et al. [32] also validate the effectiveness of directly fine-tuning from pose estimation models pre-trained on human datasets. Although progresses have been made, exiting methods still struggles to dealing with multiple animal species with large variance in appearance, texture, and pose. To address the challenge, we propose a multi-modal framework that support animal pose estimation with language descriptions of animal keypoints, by taking advantage of the abundant knowledge learned in the pre-trained vision-language models, e.g., CLIP [26].

### 2.2 Vision-language models

Vision-language models cover a wide range of research topics [31, 2, 1], while we focus on reviewing the works on vision-language pre-training and fine-tuning. Vision-language pre-training has witnessed significant progress in the last few years, which generally learns an image encoder and a text encoder jointly [26, 13, 8, 16]. A representative work is contrastive language-image pre-training dubbed CLIP [26], which uses 400 million text-image paired data acquired online to train a multi-mode pre-training model. Experiments show that CLIP can help achieve effective few-shot or even zero-shot classification by simply exploring the relations between text features and image features.

Although significant progress has been made in vision-language pre-training, how to effectively adapt these pre-trained models for downstream tasks remains to be explored. To this end, CoOp [36] and CoCoOp [37] take inspiration from prompt learning in NLP [20], and propose to utilize learnable text embedding for better image classification. Similarly, CLIP-adaptor [9] and TIP-adaptor [34] improves the model performance on downstream task through a lightweight adaptor. While the above methods focus on adapting CLIP for the image classification task, DenseCLIP [27] propose a language-guided fine-tuning method for applying the pre-trained model to dense prediction tasks, including semantic segmentation and instance segmentation. Different from these methods, we focus on utilizing the language modality in vision-language pre-trained model for better animal pose estimation through a specifically designed prompt mechanism and two contrastive loss functions.

## 3 Method

### 3.1 Preliminary: Animal pose estimation pipeline

Similar to human pose estimation task, animal pose estimation aims to locate  $N$  keypoints in the input animal instance image. We follow most of the existing pose estimation methods and apply a typical top-down keypoint detection pipeline [30, 29], which delivers better results than the bottom-up pipeline [4]. Pose estimator generally first use a detector to detect the bounding boxes of all animal instances in the image, then detect the keypoints for each animal instance. Specifically, the heatmap

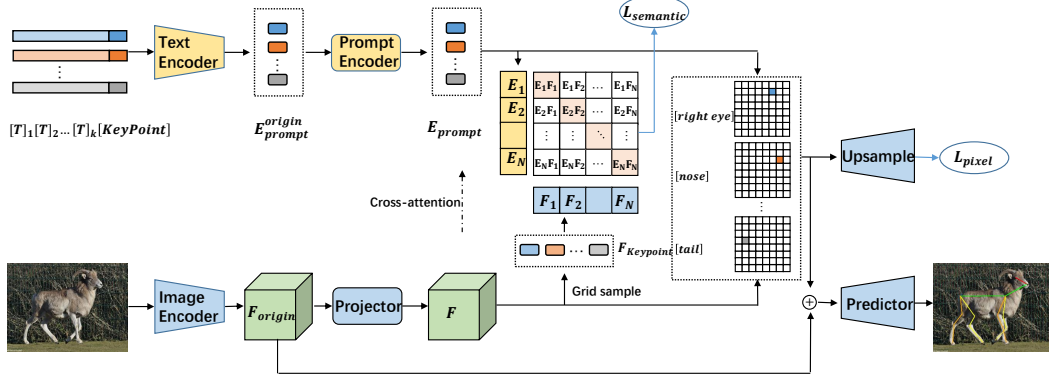


Figure 1: Illustration of the proposed PromptPose method.

representation is usually used to denote the location of each keypoint. A typical pose estimation model mainly includes two parts: image encoder and keypoint predictor. We denote as  $I \in \mathbb{R}^{h \times w \times 3}$  as the cropped instance image based on the bounding box, where  $h, w$  are the height and width of the image, respectively. The encoder  $f_{extr}$  extracts the image feature  $F \in \mathbb{R}^{h_0 \times w_0 \times C}$  from  $I$ , where  $h_0, w_0, C$  are the height, width and the number of channels, respectively. Usually, an ImageNet [5] pre-trained backbone network, e.g., ResNet-50 [12] or HRNet-32 [29], is used as the encoder. A typical ratio  $s_0$  between  $h$  and  $h_0$  is 32 for ResNet-50 and 4 for HRNet-32. Then the keypoint predictor  $f_{pred}$  decodes  $F$  into a heatmap  $H \in \mathbb{R}^{h_1 \times w_1 \times N}$ , which typically consists of several deconvolution layers depending on the ratio  $s_0$  and a convolutional prediction layer. Usually, the ratio  $s_1$  between  $h$  and  $h_1$  is 4. Finally, we get the coordinates of  $N$  keypoints  $K \in \mathbb{R}^{N \times 2}$  by applying a simple argmax operation on each heatmap and multiplying the coordinates with the scale ratio  $s_1$  to recover to the original scale:

$$K_n = s_1 \times \underset{1 \leq i \leq h_1, 1 \leq j \leq w_1}{argmax} H_n(i, j), \quad n = 1, \dots, N, \quad (1)$$

where  $K_n$  is the coordinate of  $n$ -th keypoint and  $H_n$  is  $n$ -th heatmap in  $H$ .

### 3.2 PromptPose

CLIP [26] uses “A photo of a {object}” as a template to design textual prompts, where {object} can be filled with names of different categories. By calculating the similarity between images and different textual prompts for classification, the common classification task is transformed into a contrast task and a better performance can be achieved. The form of text-image contrast designed by CLIP can handle flexible and various images and text information. Inspired by the recently introduced prompt training [20] and CLIP[26], we propose the PromptPose, which includes a novel language prompt, a pixel-level contrastive loss, and a semantic-level text-image contrast loss, to adapt the language knowledge to animal pose estimation. Fig. 1 shows an overview of the proposed PromptPose method.

#### 3.2.1 Language prompt design

According to the characteristics of pose estimation, we designed novel textual prompts to better adapt CLIP. In particular, different from CLIP, pose estimation does not depend on specific categories and requires to find the position of a set of keypoints for each image. Accordingly, we fill in {object} with the names of different keypoints like ‘nose’ to get  $N$  textual prompts, where  $N$  is the number of keypoints. Based on CoOp [36], we use a learnable template of length  $k$  instead of the fixed template in CLIP to make the prompt better adapt to pose estimation, obtaining the prompt as follows:

$$p_n = [T]_1[T]_2 \dots [T]_k[KeyPoint]_n, \quad n = 1, \dots, N, \quad (2)$$

where  $[T]_i, i \in \{1, 2, \dots, k\}$  represents the learnable template and  $[KeyPoint]_n$  represents the  $i$ -th keypoint name. The  $N$  textual prompts are mapped to the multi-modal embedding space by using a CLIP pre-trained text encoder to get the prompt embedding  $E_{prompt}^{origin} \in \mathbb{R}^{N \times C_{emb}}$ . Considering the intrinsic relationship between different keypoints is important for pose estimation, we further propose

a lightweight prompt encoder (*i.e.*, a single transformer layer) to model the relationship between different keypoint prompt embeddings and promote their interactions, and use cross-attention to enhance prompt embeddings with the image feature [27], getting the enhanced prompt embeddings  $E_{prompt} \in \mathbb{R}^{N \times C_{emb}}$ .

### 3.2.2 Pixel-level contrast

In order to utilize pose-related semantics in the language model to perform pose estimation, we introduce a pixel-level contrast to construct dense connections between prompt embeddings and the image feature. Specifically, we formulate that the input image is passed through the image encoder to obtain the image feature  $F_{origin} \in \mathbb{R}^{H \times W \times C}$ , where  $H$ ,  $W$ ,  $C$  are the height, width, and the number of channels, respectively. Then the obtained  $F_{origin}$  is mapped to the multi-modal embedding space through a projector, obtaining  $F \in \mathbb{R}^{H \times W \times C_{emb}}$ . For different image encoders, we employ slightly different projectors. For example, for a ViT [6] backbone encoder, the projector is a linear projection layer, while for the ResNet [12] backbone encoder, the projector contains a global average pooling layer, a multi-head self-attention (MHSA) layer, and a linear projection layer, following the design in CLIP [26]. After the image feature and textual prompts are mapped to the multi-modal embedding space, we apply inner product to the normalized prompt embedding and image feature and get the text-pixel matching score of each spatial position:

$$S_{ijn} = F_{ij} \cdot E_{prompt}^n, \quad i = 1, \dots, H; j = 1, \dots, W; n = 1, \dots, N, \quad (3)$$

where  $F_{ij} \in \mathbb{R}^{1 \times C_{emb}}$  is the feature vector of  $F$  at pixel  $(i, j)$ , and  $E_{prompt}^n$  is the  $n$ -th prompt embedding. Accordingly, we can get the pixel-level matching score map

$$S = \{S_{ijn}\}_{i,j,n=1,1,1}^{H,W,N} \in \mathbb{R}^{H \times W \times N} \quad (4)$$

for  $N$  prompt embeddings. This score map is supervised by the target heatmap  $H_{target}$  after deconvolutional layers for upsampling, through the pixel-level contrastive loss defined as:

$$\mathcal{L}_{pixel} = MSE(S, H_{target}), \quad (5)$$

where  $MSE$  is the mean squared error loss.

### 3.2.3 Semantic-level contrast

Although we can establish dense connections between text and image through the pixel-level contrast, this connection requires text and pixel-level image features to be in a compatible multi-modal embedding space. The existing image-text contrastive pre-training [26] only matches the semantics of text and image in a global manner, and there is still a gap to the local pixel-level connection we need to establish. In this regard, we propose a semantic-level contrast close to pre-training to bridge the gap between text and local keypoint features. Specifically, during the training process, we use the ground truth locations of the keypoint  $K \in \mathbb{R}^{N \times 2}$  to perform grid sampling on  $F$  to obtain the local features of  $N$  keypoints:

$$F_{keypoint} = \{F_n | n = 1, \dots, N\} \in \mathbb{R}^{N \times C_{emb}}. \quad (6)$$

Then, we calculate the semantic matching score map between the local feature of keypoints and prompt embeddings as follows:

$$M = \hat{F}_{keypoint} \hat{E}_{prompt}^T \in \mathbb{R}^{N \times N}, \quad (7)$$

where  $\hat{F}_{keypoint}$  and  $\hat{E}_{prompt}$  are normalized local keypoint features and prompt embeddings, respectively. We keep  $F_{keypoint}$ ,  $E_{prompt}$  and the ground truth label  $K$  in the same order in dimension  $N$ , and the matching target  $M_{label}$  can be obtained as  $[0, 1, 2, \dots, N - 1]$ . We perform contrastive learning on both of prompt embedding and keypoint feature based on the semantic-level contrastive loss defined as follows:

$$\mathcal{L}_{semantic} = \frac{1}{2}(CE(M, M_{label}) + CE(M^T, M_{label})), \quad (8)$$

where  $CE$  represents the cross entropy classification loss. This semantic-level contrast can promote the local keypoint feature and prompt embedding aligning in a compatible multi-modal embedding space, effectively narrowing the gap between the global contrast in pre-training and the local contrast in pose estimation.

### 3.2.4 Final Prediction and Learning Objective

The pixel-level contrast establishes a dense connection between the textual prompt and the image feature, while the designed semantic-level contrast narrows the gap between the pre-trained global contrast and the local contrast of pose estimation. Therefore, we can take advantage of the established text-image connection to utilize the rich semantic information related to pose in the language model, making it able to help our model understand variable animal poses. To this end, we fuse the pixel-level matching score map, which contains the text-image connection information, with the image feature  $F_{origin}$  to obtain  $F_{fuse}$  as follows:

$$F_{fuse} = F_{origin} \oplus S \in \mathbb{R}^{H \times W \times (C+N)}, \quad (9)$$

where  $\oplus$  represents the concatenate operation. Then,  $F_{fuse}$  is fed into a keypoint predictor to predict the pose heatmap, which is supervised by the prediction loss  $\mathcal{L}_{pred}$ , defined as the *MSE* loss between the predicted heatmap and groundtruth heatmap. The overall training loss can be written as:

$$\mathcal{L}_{total} = \mathcal{L}_{pred} + \alpha_1 \cdot \mathcal{L}_{semantic} + \alpha_2 \cdot \mathcal{L}_{pixel}, \quad (10)$$

where  $\alpha_1$  and  $\alpha_2$  are two hyper-parameters to balance the importance of  $\mathcal{L}_{semantic}$  and  $\mathcal{L}_{pixel}$ .

## 4 Experiments

### 4.1 Experimental setup

**Datasets and evaluation metrics** For evaluation, we mainly conducted experiments on AP-10K [32], which is the existing largest animal pose estimation benchmark. AP-10K contains 10,015 images collected and filtered from 23 animal families and 54 species, containing rich diversity of animal species. Similar to the keypoint definition for human pose estimation, 17 keypoints are defined to represent animal pose, containing two eyes, one nose, one neck, two shoulders, two elbows, two knees, two hips, four paws and one tail. Following the supervised learning setting in AP-10K, we conduct training on the training set (7k images) and report results on the validation set (1k images).

In addition to AP-10K, we also attempt to study the effects of transferring the knowledge from human pose estimation models to the animal pose estimation model with the help of our PromptPose framework. We use the MS COCO 2017 [18] training set as the human pose dataset for pre-training, and further finetune the pre-trained model under the PromptPose framework on AP-10K to test the knowledge transfer performance. The COCO dataset contains more than 200,000 images and 250,000 human instances which are labeled with 17 keypoints. For all the evaluation, we adopt the Average Precision (AP) based on Object Keypoint Similarity (OKS) as the main evaluation metric on the AP-10K dataset. The detailed protocol definitions can be found in [17].

**Implementation details** In this paper, we follow the widely used two-stage top-down pose estimation paradigm similar to SimpleBaseline [30]. We adopt the ground truth bounding box annotations in AP-10k to crop animal instances into test images following [32]. For the image encoder in the pose estimation pipeline, we select the widely used ResNet [12] and the recently introduced attention-based visual transformer ViT [6] as backbones, *i.e.*, ResNet-50 and ViT-Base. We use ImageNet [5] and CLIP [26] as visual and language-image pre-training datasets, respectively. We adopt the text encoder of CLIP-ResNet-50 and CLIP-ViT-Base as our language models and initialize them with the corresponding CLIP pre-trained weights. The keypoints are predicted from the heatmaps following SimpleBaseline [30]. We train the models on 8 NVIDIA A100 GPUs.

During training, we follow most of the training settings in AP-10K, *i.e.*, the input image of each instance was cropped and resized to  $256 \times 256$ , followed by random flip, rotation and scale jitter. Each model is trained for a total of 210 epochs with a step-wise learning rate schedule which drops by 0.1 times at the 170th and 200th epoch, respectively. We use the AdamW [21] optimizer with a weight decay of  $1e-4$ . For supervised learning on AP-10K, we train the model with a batch size of 128 and set  $5e-4$  as the initial learning rate for both ResNet-50 and ViT-Base, but use a smaller initial learning rate of  $5e-5$  to ViT-Base backbone to prevent overfitting. For few-shot learning on AP-10K, we adopt a batch size of 64 and set the initial learning rate to  $5e-4$  and  $5e-5$  for ResNet-50 and ViT-Base, respectively. When pre-training on COCO, we train the model for a total of 210 epochs and use a step-wise learning rate schedule. We train our model with a batch size of 512 and set the initial learning rate to  $5e-4$  and  $2e-4$  for ResNet and ViT-Base, respectively. After pre-training, we

Table 1: Performance comparison on AP-10K.

Method	Backbone	Pre-train	$AP$	$AP_{50}$	$AP_{75}$	$AP_M$	$AP_L$	$AR$
SimpleBaseline	ResNet-50	ImageNet	70.2	94.2	76.0	45.5	70.4	73.5
SimpleBaseline	ResNet-50	CLIP	70.9	94.6	76.8	44.8	71.2	74.1
PromptPose (ours)	ResNet-50	CLIP	72.9	95.4	79.4	43.2	73.2	76.3
SimpleBaseline	ViT-Base	CLIP	72.6	94.7	79.5	43.4	72.8	75.8
PromptPose (ours)	ViT-Base	CLIP	73.1	95.0	79.8	47.9	73.2	76.3

Table 2: 20-shot performance comparison on AP-10K.

Method	Backbone	Pre-train	$AP$	$AP_{50}$	$AP_{75}$	$AP_M$	$AP_L$	$AR$
SimpleBaseline	ResNet-50	ImageNet	51.1	85.4	50.2	26.7	51.3	56.3
SimpleBaseline	ResNet-50	CLIP	51.8	84.3	52.5	26.1	52.0	56.9
PromptPose (ours)	ResNet-50	CLIP	54.0	85.9	56.2	26.4	54.2	58.9
SimpleBaseline	ViT-Base	CLIP	57.4	88.9	61.2	20.9	57.8	61.2
PromptPose (ours)	ViT-Base	CLIP	58.6	89.5	61.3	24.9	58.9	62.6

finetune the model on AP-10K. For supervised learning, we train our model with a batch size of 128 and set  $6e-4$  and  $5e-5$  as the learning rate for ResNet-50 and ViT-Base, respectively. For few-shot learning, we adopt a batch size of 64 and a learning rate of  $5e-4$  for ResNet-50, and a batch size of 128 and a learning rate of  $5e-5$  for ViT-Base. In all language-driven experiments, we freeze the text encoder to maintain language knowledge and prevent from being distracted.

## 4.2 Results and analysis

### 4.2.1 Experiments on AP-10K

**Supervised learning** The results under supervised learning setting on AP-10K are shown in Table 1. We can first find that SimpleBaseline with a ResNet-50 backbone pre-trained on CLIP obtains 1% AP higher than the counterpart with the ImageNet pre-trained weight. This illustrates that the language knowledge learned with CLIP can already bring improvements on animal pose estimation. Furthermore, by applying the proposed PromptPose, we achieve the better AP using the ResNet-50 backbone with a gain of another 2 points in AP than the CLIP model. Using the more powerful ViT backbone, the PromptPose achieves the best performance, demonstrating that PromptPose is effective to adapt rich language knowledge to animal pose data for improving pose estimation performance.

**Few-shot learning** We also present few-shot learning performance to study the generalizability of different methods. We randomly selected 20 samples for each species in the training set to form a 20-shot animal pose estimation training set, and the model is tested on the validation set to evaluate the performance of models trained under the challenging training setting with a smaller amount of training data available. The results are shown in Table 2. Similar with supervised learning, SimpleBaseline with a ResNet-50 backbone pre-trained on CLIP has better performance than the ImageNet pre-trained counterpart, with an improvement of 0.7% in AP. Also, PromptPose still outperform SimpleBaseline by a large margin, *i.e.*, 54.0 AP vs. 51.8 AP for ResNet-50, and 58.6 AP vs. 57.4 AP for ViT-Base, respectively.

### 4.2.2 Improvement on transfer learning from COCO to AP-10K.

Using PromptPose, we further show that the human pose knowledge can be better transferred to the animal pose estimation. To verify our model’s ability to improve human pose knowledge transfer, we introduce an additional pre-training procedure using MS COCO human pose dataset before the finetuning on AP-10K which follows the experiment setting in the previous section. The results of supervised learning and few shot learning are shown in Table 3 and Table 4, respectively. From the results, we can generally observe that human pose knowledge learned during the pre-training stage is helpful for animal pose estimation, which improves all the models on animal pose estimation. For example, for the SimpleBaseline with the ImageNet pre-trained ResNet-50 backbone, pre-training on

Table 3: Performance comparison of transfer learning

from MS COCO to AP-10K under the supervised learning setting.

Method	Backbone	Pre-train	$AP$	$AP_{50}$	$AP_{75}$	$AP_M$	$AP_L$	$AR$	Human AP
SimpleBaseline	ResNet-50	ImageNet	72.4	94.8	78.2	43.2	72.6	75.6	71.8
SimpleBaseline	ResNet-50	CLIP	74.4	95.7	81.0	43.4	74.7	77.6	72.7
PromptPose (ours)	ResNet-50	CLIP	75.2	96.1	81.4	47.5	75.5	78.5	73.0
SimpleBaseline	ViT-Base	CLIP	73.9	95.4	80.9	49.2	74.1	77.2	73.2
PromptPose (ours)	ViT-Base	CLIP	74.2	95.4	80.4	47.3	74.4	77.5	73.3

Table 4: Performance comparison of transfer learning from MS COCO to AP-10K under the 20-shot learning setting.

Method	Backbone	Pre-train	$AP$	$AP_{50}$	$AP_{75}$	$AP_M$	$AP_L$	$AR$	Human AP
SimpleBaseline	ResNet-50	ImageNet	60.7	88.4	65.2	29.9	61.0	65.1	71.8
SimpleBaseline	ResNet-50	CLIP	62.4	90.4	67.1	34.1	62.7	66.4	72.7
PromptPose (ours)	ResNet-50	CLIP	62.6	90.2	66.9	30.1	62.9	66.8	73.0
SimpleBaseline	ViT-Base	CLIP	63.8	91.0	69.2	36.5	64.0	67.5	73.2
PromptPose (ours)	ViT-Base	CLIP	64.1	91.9	68.4	35.5	64.3	67.7	73.3

human pose data helps improve 2.2 AP points under supervised learning, from 70.2 AP in Table 1 to 72.4 AP in Table 3, and 9.6 AP points under 20-shot learning, from 51.1 AP in Table 2 to 60.7 AP in Table 4. In addition, using the CLIP pre-trained backbone, the performance can be further improved, validating the proposed idea that the cross-modal feature representation facilitates knowledge transfer since both human and animal share some keypoint text description, *e.g.*, nose and eyes. Moreover, with the proposed PromptPose, the performance can be further improved, *e.g.*, from 74.4 AP to 75.2 AP under supervised learning, which matches the previous best 75.3 AP obtained by the stronger HRNet model that has also been pretrained on MS COCO human pose data [32]. The results validate the effectiveness of our PromptPose for knowledge transfer, where the prompt encoder could provide an explicit connection between human and animal in the form of shared text description of keypoints.

In addition, we also try to investigate the influence of our PromptPose method on the human pose estimation task. The ‘‘Human AP’’ in the Table 3 shows the results on the MS COCO val set for human pose estimation. To perform human pose estimation, it is worth mentioning that we only need to replace  $[KeyPoint]$  in Eq. (2) with human keypoint names. The results show that PromptPose is still effective for improving human pose estimation but the benefit is marginal especially for the ViT backbone. We analyze that this is because human pose training data are sufficient to train a good model with promising performance, thus the benefit of introducing language knowledge is smaller comparing to the animal pose estimation task where much less training data are available.

### 4.3 Ablation study

**Pixel-level contrastive loss** In the PromptPose framework, the pixel-level contrastive loss promotes the alignment of text embedding and image feature belonging to the keypoint regions and pushes away text embedding and image feature belonging to non-keypoint regions or background, *i.e.*, *prompting to learn image feature of keypoint via text description*. To study the impact of pixel-level contrastive loss, we only use the pixel-level contrastive loss on the SimpleBaseline with CLIP pre-trained ResNet-50 backbone. As shown in Table 5, it improves the performance from 70.9 AP to 72.1 AP.

**Semantic-level contrastive loss** Since CLIP pre-training matches the semantics of text and image in a global manner, while pixel-level contrast requires that the semantics of text and image match in local, the semantic-level contrast is designed to bridge the gap between pose estimation and pre-training. As shown in Table 5, the semantic-level contrastive loss further improves the performance by 0.5 AP. Since the grid sampling in Eq. (6) and semantic-level contrastive loss have no trainable parameters, it only brings marginal computational cost during training and no computational cost during inference.

**Prompt encoder** From Table 5, we can see that the prompt encoder further brings 0.2 AP improvement in AP, demonstrating the value of modeling the semantic relationship of keypoints for facilitating prompting. Note that the prompt encoder is very lightweight and only has a single transformer layer.



Table 5: Ablation study of PromptPose with a CLIP pre-trained ResNet-50 backbone on AP-10K.

$\mathcal{L}_{pixel}$	$\mathcal{L}_{semantic}$	$PromptEncoder$	AP	AR
×	×	×	70.9	74.1
✓	×	×	72.1	75.3
✓	✓	×	72.6	75.8
✓	×	✓	72.3	75.6
✓	✓	✓	72.9	76.3

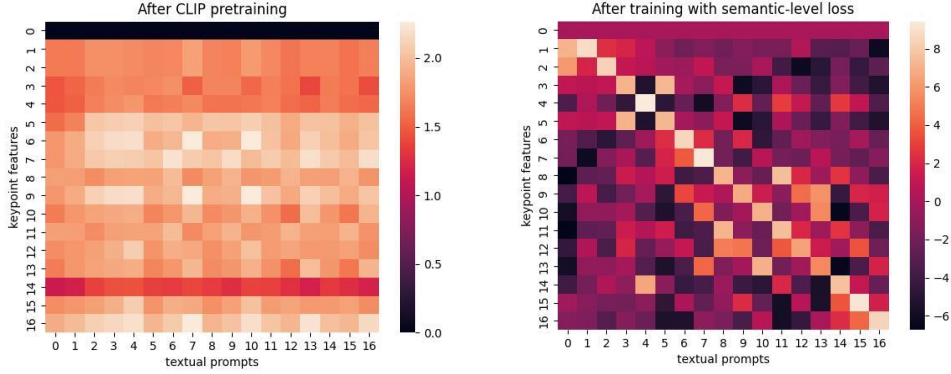


Figure 2: Visualization of semantic-level contrast score map. For each grid-sampled local keypoint feature, we calculate its similarity with different textual prompts after CLIP pre-training and after finetuning with the semantic-level loss, and show the score map on the left and right, respectively. Note that the left eye (*i.e.*, the first keypoint) of the animal is invisible in the test image.

#### 4.4 Visualization and analysis

**Semantic-level contrast:** Based on Eq. (7), we obtained the similarities between textual prompts and local keypoint features before and after finetuning with semantic-level loss  $\mathcal{L}_{semantic}$ . From Fig. 2, we can see that after CLIP pre-training, each keypoint feature has almost the same similarity for different textual prompts. However, after finetuning with  $\mathcal{L}_{semantic}$ , each local keypoint feature has the highest similarity with the corresponding textual prompt (*i.e.*, the diagonal elements). It shows CLIP pre-training only establishes the global semantic connection between text and image, while  $\mathcal{L}_{semantic}$  helps establish explicit correspondence between text and visual feature of each keypoint.

**Qualitative analysis** We also present some visual results of PromptPose and SimpleBaseline in the supplementary material, which also show the superiority of PromptPose owing to language prompt.

## 5 Conclusion and discussion

Researches on animal pose estimation are hindered by small dataset and large variance. To tackle this, we propose a novel framework, termed PromptPose, to effectively utilize language models for better animal poses estimation. Within the framework, we make two technical contributions aiming to adapt the language knowledge to the visual animal poses, including a semantic-level and a pixel-level text-image contrastive loss. Besides, a prompt encoder is introduced to emphasize the correlation between different text keypoint embeddings. Experiments on both supervised and few-shot settings validate the effectiveness of the proposed method. As the first study of cross-modal animal pose estimation, we hope it can provide useful insights to and draw attentions from the research community on improving animal pose estimation with multi-modal knowledge.

**Limitation discussion** In this study, we only validate the effectiveness of PromptPose in the top-down pose estimation pipeline, where only a single animal instance is in the input image. However, in the bottom-up pipeline, there may be many animal instances, *i.e.*, implying a large number of

keypoints, therefore, abundant text-image contrastive signals could be established, probably helping learn more discriminative feature representations and achieve better performance.

**Social impact** PromptPose relies on a pre-trained cross-modal model which may learn biased representation due to the data bias, leading to incorrect predictions, *e.g.*, on animal-like images. Besides, pre-training large cross-modal model like CLIP always requires a large amount of computational resources and increases carbon emissions. Further efforts should be made to address these issues.

## References

- [1] P. Anderson, Q. Wu, D. Teney, J. Bruce, M. Johnson, N. Sünderhauf, I. Reid, S. Gould, and A. Van Den Hengel. Vision-and-language navigation: Interpreting visually-grounded navigation instructions in real environments. In *Proceedings of the IEEE conference on computer vision and pattern recognition*, pages 3674–3683, 2018.
- [2] S. Antol, A. Agrawal, J. Lu, M. Mitchell, D. Batra, C. L. Zitnick, and D. Parikh. Vqa: Visual question answering. In *Proceedings of the IEEE international conference on computer vision*, pages 2425–2433, 2015.
- [3] J. Cao, H. Tang, H.-S. Fang, X. Shen, C. Lu, and Y.-W. Tai. Cross-domain adaptation for animal pose estimation. In *Proceedings of the IEEE/CVF International Conference on Computer Vision*, pages 9498–9507, 2019.
- [4] Z. Cao, T. Simon, S.-E. Wei, and Y. Sheikh. Realtime multi-person 2d pose estimation using part affinity fields. In *Proceedings of the IEEE conference on computer vision and pattern recognition*, pages 7291–7299, 2017.
- [5] J. Deng, W. Dong, R. Socher, L.-J. Li, K. Li, and L. Fei-Fei. Imagenet: A large-scale hierarchical image database. In *2009 IEEE conference on computer vision and pattern recognition*, pages 248–255. Ieee, 2009.
- [6] A. Dosovitskiy, L. Beyer, A. Kolesnikov, D. Weissenborn, X. Zhai, T. Unterthiner, M. Dehghani, M. Minderoer, G. Heigold, S. Gelly, et al. An image is worth 16x16 words: Transformers for image recognition at scale. *arXiv preprint arXiv:2010.11929*, 2020.
- [7] H.-S. Fang, S. Xie, Y.-W. Tai, and C. Lu. Rmpe: Regional multi-person pose estimation. In *Proceedings of the IEEE international conference on computer vision*, pages 2334–2343, 2017.
- [8] A. Fürst, E. Rumetshofer, V. Tran, H. Ramsauer, F. Tang, J. Lehner, D. Kreil, M. Kopp, G. Klambauer, A. Bitto-Nemling, et al. Cloob: Modern hopfield networks with infoloob outperform clip. *arXiv preprint arXiv:2110.11316*, 2021.
- [9] P. Gao, S. Geng, R. Zhang, T. Ma, R. Fang, Y. Zhang, H. Li, and Y. Qiao. Clip-adapter: Better vision-language models with feature adapters. *arXiv preprint arXiv:2110.04544*, 2021.
- [10] Z. Geng, K. Sun, B. Xiao, Z. Zhang, and J. Wang. Bottom-up human pose estimation via disentangled keypoint regression. In *Proceedings of the IEEE/CVF Conference on Computer Vision and Pattern Recognition*, pages 14676–14686, 2021.
- [11] J. M. Graving, D. Chae, H. Naik, L. Li, B. Koger, B. R. Costelloe, and I. D. Couzin. Deepposekit, a software toolkit for fast and robust animal pose estimation using deep learning. *Elife*, 8:e47994, 2019.
- [12] K. He, X. Zhang, S. Ren, and J. Sun. Deep residual learning for image recognition. In *Proceedings of the IEEE conference on computer vision and pattern recognition*, pages 770–778, 2016.
- [13] C. Jia, Y. Yang, Y. Xia, Y.-T. Chen, Z. Parekh, H. Pham, Q. Le, Y.-H. Sung, Z. Li, and T. Duerig. Scaling up visual and vision-language representation learning with noisy text supervision. In *International Conference on Machine Learning*, pages 4904–4916. PMLR, 2021.
- [14] C. Li and G. H. Lee. From synthetic to real: Unsupervised domain adaptation for animal pose estimation. In *Proceedings of the IEEE/CVF Conference on Computer Vision and Pattern Recognition*, pages 1482–1491, 2021.
- [15] S. Li, J. Li, H. Tang, R. Qian, and W. Lin. Atrw: A benchmark for amur tiger re-identification in the wild. In *Proceedings of the 28th ACM International Conference on Multimedia*, pages 2590–2598, 2020.
- [16] Y. Li, F. Liang, L. Zhao, Y. Cui, W. Ouyang, J. Shao, F. Yu, and J. Yan. Supervision exists everywhere: A data efficient contrastive language-image pre-training paradigm. *arXiv preprint arXiv:2110.05208*, 2021.
- [17] Y. Li, S. Zhang, Z. Wang, S. Yang, W. Yang, S.-T. Xia, and E. Zhou. Tokenpose: Learning keypoint tokens for human pose estimation. In *Proceedings of the IEEE/CVF International Conference on Computer Vision*, pages 11313–11322, 2021.
- [18] T.-Y. Lin, M. Maire, S. Belongie, J. Hays, P. Perona, D. Ramanan, P. Dollár, and C. L. Zitnick. Microsoft coco: Common objects in context. In *European conference on computer vision*, pages 740–755. Springer, 2014.
- [19] J.-J. Liu, Q. Hou, M.-M. Cheng, C. Wang, and J. Feng. Improving convolutional networks with self-calibrated convolutions. In *Proceedings of the IEEE/CVF Conference on Computer Vision and Pattern Recognition*, pages 10096–10105, 2020.
- [20] P. Liu, W. Yuan, J. Fu, Z. Jiang, H. Hayashi, and G. Neubig. Pre-train, prompt, and predict: A systematic survey of prompting methods in natural language processing. *arXiv preprint arXiv:2107.13586*, 2021.
- [21] I. Loshchilov and F. Hutter. Decoupled weight decay regularization. *arXiv preprint arXiv:1711.05101*, 2017.

- [22] A. Mathis, T. Biasi, S. Schneider, M. Yuksekgonul, B. Rogers, M. Bethge, and M. W. Mathis. Pretraining boosts out-of-domain robustness for pose estimation. In *Proceedings of the IEEE/CVF Winter Conference on Applications of Computer Vision*, pages 1859–1868, 2021.
- [23] J. Mu, W. Qiu, G. D. Hager, and A. L. Yuille. Learning from synthetic animals. In *Proceedings of the IEEE/CVF Conference on Computer Vision and Pattern Recognition*, pages 12386–12395, 2020.
- [24] A. Newell, Z. Huang, and J. Deng. Associative embedding: End-to-end learning for joint detection and grouping. *Advances in neural information processing systems*, 30, 2017.
- [25] A. Newell, K. Yang, and J. Deng. Stacked hourglass networks for human pose estimation. In *European conference on computer vision*, pages 483–499. Springer, 2016.
- [26] A. Radford, J. W. Kim, C. Hallacy, A. Ramesh, G. Goh, S. Agarwal, G. Sastry, A. Askell, P. Mishkin, J. Clark, et al. Learning transferable visual models from natural language supervision. In *International Conference on Machine Learning*, pages 8748–8763. PMLR, 2021.
- [27] Y. Rao, W. Zhao, G. Chen, Y. Tang, Z. Zhu, G. Huang, J. Zhou, and J. Lu. Denseclip: Language-guided dense prediction with context-aware prompting. *arXiv preprint arXiv:2112.01518*, 2021.
- [28] A. Sanakoyeu, V. Khalidov, M. S. McCarthy, A. Vedaldi, and N. Neverova. Transferring dense pose to proximal animal classes. In *Proceedings of the IEEE/CVF Conference on Computer Vision and Pattern Recognition*, pages 5233–5242, 2020.
- [29] J. Wang, K. Sun, T. Cheng, B. Jiang, C. Deng, Y. Zhao, D. Liu, Y. Mu, M. Tan, X. Wang, et al. Deep high-resolution representation learning for visual recognition. *IEEE transactions on pattern analysis and machine intelligence*, 43(10):3349–3364, 2020.
- [30] B. Xiao, H. Wu, and Y. Wei. Simple baselines for human pose estimation and tracking. In *Proceedings of the European conference on computer vision (ECCV)*, pages 466–481, 2018.
- [31] K. Xu, J. Ba, R. Kiros, K. Cho, A. Courville, R. Salakhudinov, R. Zemel, and Y. Bengio. Show, attend and tell: Neural image caption generation with visual attention. In *International conference on machine learning*, pages 2048–2057. PMLR, 2015.
- [32] H. Yu, Y. Xu, J. Zhang, W. Zhao, Z. Guan, and D. Tao. Ap-10k: A benchmark for animal pose estimation in the wild. *arXiv preprint arXiv:2108.12617*, 2021.
- [33] J. Zhang, Z. Chen, and D. Tao. Towards high performance human keypoint detection. *International Journal of Computer Vision*, 129(9):2639–2662, 2021.
- [34] R. Zhang, R. Fang, P. Gao, W. Zhang, K. Li, J. Dai, Y. Qiao, and H. Li. Tip-adapter: Training-free clip-adapter for better vision-language modeling. *arXiv preprint arXiv:2111.03930*, 2021.
- [35] C. Zheng, W. Wu, T. Yang, S. Zhu, C. Chen, R. Liu, J. Shen, N. Kehtarnavaz, and M. Shah. Deep learning-based human pose estimation: A survey. *arXiv preprint arXiv:2012.13392*, 2020.
- [36] K. Zhou, J. Yang, C. C. Loy, and Z. Liu. Learning to prompt for vision-language models. *arXiv preprint arXiv:2109.01134*, 2021.
- [37] K. Zhou, J. Yang, C. C. Loy, and Z. Liu. Conditional prompt learning for vision-language models. *arXiv preprint arXiv:2203.05557*, 2022.

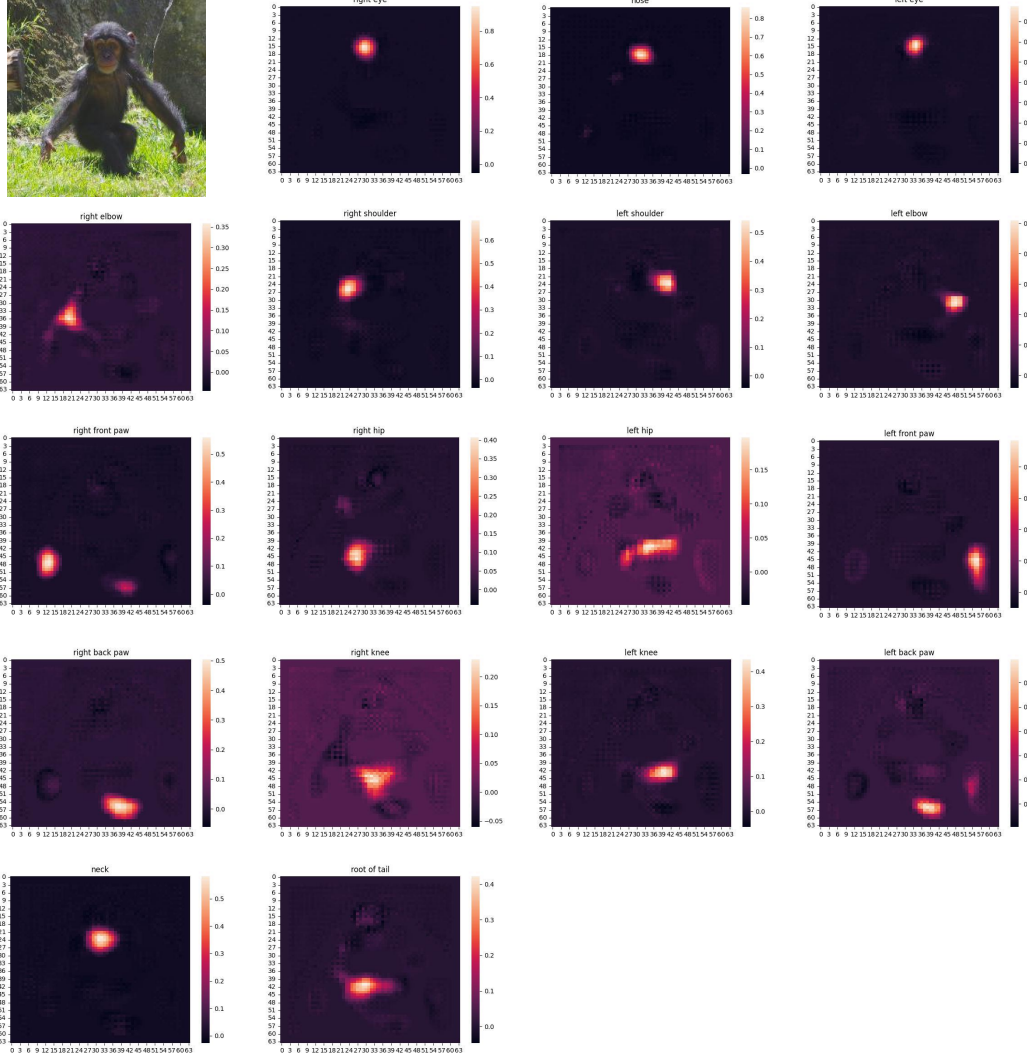


Figure 3: Visualization of the pixel-level score maps obtained after training with pixel-level contrastive loss in PromptPose. The score maps for different keypoints are displayed in the following order: right eye, nose, left eye, right elbow, right shoulder, left shoulder, left elbow, right front paw, right hip, left hip, left front paw, right back paw, right knee, left knee, left back paw, neck, root of tail (from the first row to the last row, from left to right in each row).

## 6 Supplementary Material

In the supplementary material, we first visualize the pixel-level score map to explicitly demonstrate the role of pixel-level contrast in PromptPose. Then we show some pose estimation results for SimpleBaseline [30] and PromptPose for qualitative analysis, which shows the superiority of the proposed PromptPose.

### 6.1 Visualization of Pixel-level Contrast

In order to study the effect of the pixel-level contrast, we obtain the pixel-level score map according to Eq.(3) and Eq.(4) in the main text. After upsampling the score map, we visualized the score map as shown in Fig. 3. From left to right and from top to bottom, we get 17 score maps for the right eye, nose, left eye, right elbow, right shoulder, left shoulder, left elbow, right front paw, right hip, left hip, left front paw, right back paw, right knee, left knee, left back paw, neck, and root of tail, respectively. It can be seen that for each prompt embedding, the highest score values show up in the image region of the corresponding keypoint. This indicates that the model can well-capture the similarity between the prompt embedding and the corresponding keypoint regions.

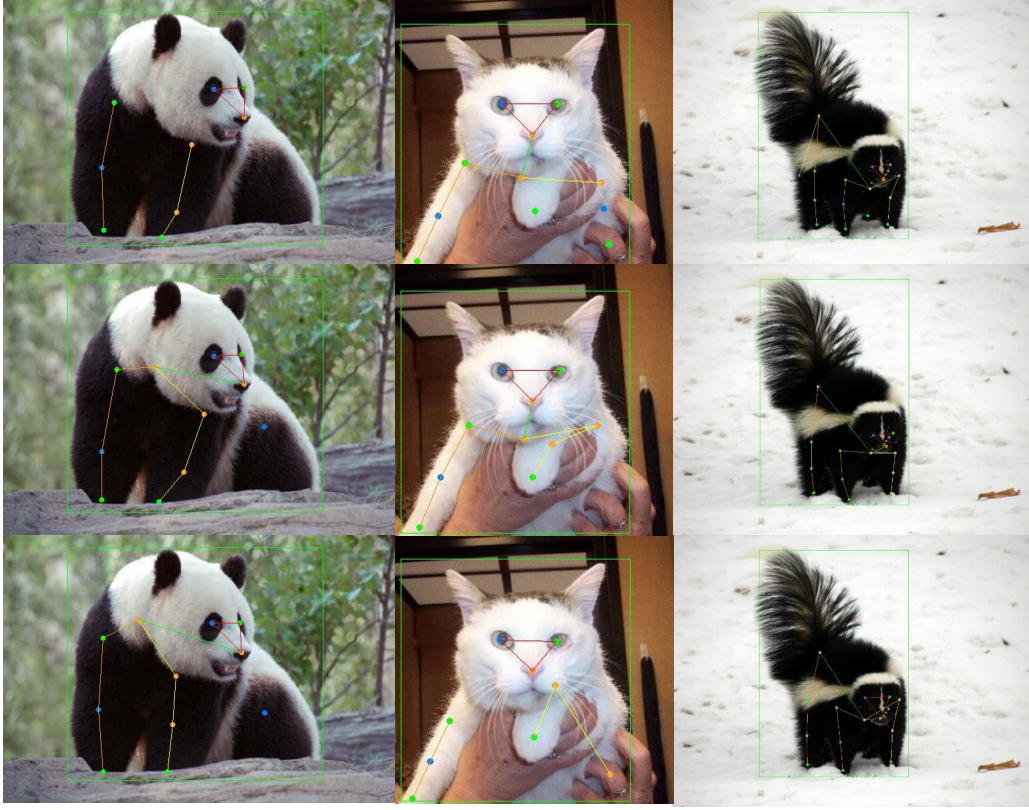


Figure 4: Qualitative analysis of the proposed PromptPose (the second row) and the SimpleBaseline [30] (the first row). The ground truth poses are shown in the last row.

Thereby, the associations between language descriptions and image features are established, which helps the model locate each keypoint for better pose estimation.

## 6.2 Qualitative Analysis

To get an intuitive understanding of the proposed method, we propose some qualitative results in Fig. 4 and Fig. 5. In each figure, the baseline method, i.e. SimpleBaseline [30], the proposed PromptPose, and the ground truth are shown from top to bottom. As can be seen, our method can produce accurate pose estimation results on animals with significant variance in appearances and poses. Taking the first column in Fig. 4 as an example, the baseline method in the first row overlooks the neck and left hip of the panda. By contrast, our PromptPose successfully leverages the prompting ability of language description and outputs all keypoints that are labeled in the ground truth. Similar observations can also be made from demo images of other animal species. Besides, PromptPose can sometimes produce more accurate results than the human annotation. For example, in the second column, the neck, the left elbow, and the left shoulder are neglected or mistaken in the ground truth. By contrast, our PromptPose can locate and recognize those keypoints, demonstrating its potential of alleviating human labor in real-world applications.



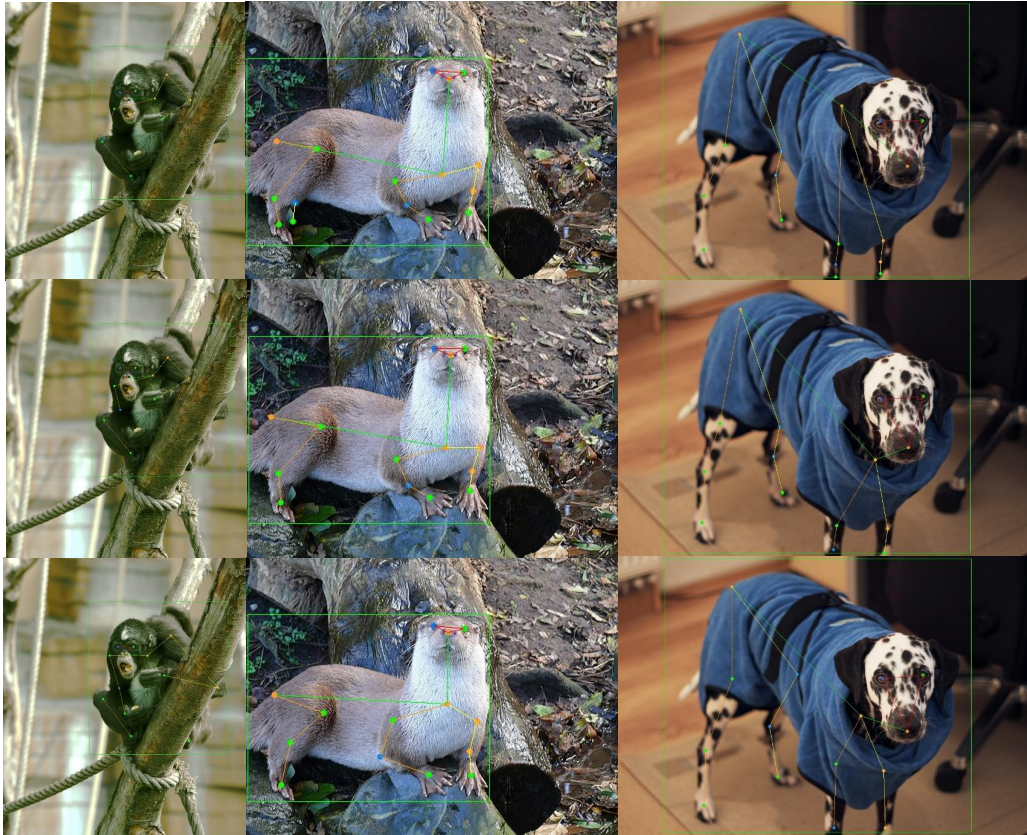


Figure 5: More qualitative results of the proposed PromptPose (the second row) and the SimpleBaseline [30] (the first row). The ground truth poses are shown in the last row.